Regular Article

Journal of the Vacuum Society of Japan Vol. 55, No. 3 (2012)

Panel Processing Effects on Discharge Characteristics of Plasma Display Panels

Takanobu YANO*1, Kazuya UCHIDA*1, Giichiro UCHIDA*2 †1,
Tsutae SHINODA*2 and Hiroshi KAJIYAMA*2

*1*Tsukuba Institute for Super Materials, ULVAC, Inc., 5–9–6 Tohkohdai, Tsukuba, Ibaraki 300–2635, Japan*
*2*Graduate School of Advanced Sciences of Matter, Hiroshima University, 1–3–1 Kagamiyama, Higashi-hiroshima, Hiroshima 739–8530, Japan*

(Received September 27, 2011, Accepted November 15, 2011)

We developed a new PDP manufacturing method in which protective layer deposition and sealing were performed continuously in high vacuum (pressure range 10^{-6} Pa), to keep the protective layer surface as clean as possible (''all-in-vacuum''). The ''all-in-vacuum'' panel shows high performance: 1) short aging time, 2) low firing voltage, and 3) short statistical time lag. Especially, the short statistical time lag is not obtained once the MgO layer is annealed in ambient air, even though the annealed MgO layer is activated in high vacuum.

1. Introduction

AC Plasma display panels (AC–PDPs) are widely used as flat panel displays (FPDs) because of their excellent potential for high-definition television with high brightness, fast response and wide-view angle performance. For further penetration to the FPD market, it is necessary to improve their luminance and luminous efficacy. The protective layer in PDPs is a key material to reduce the firing voltage by secondary electron emission. Actually, MgO film has been used as a protective layer because of its high secondary electron emission coefficient (γ) and high durability against ion bombardment[1,2].

Reportedly, the luminous efficacy is improved by the use of a discharge gas with higher Xe content[3]. The subeffect is that the discharge voltage increases with high Xe gas[3]. High γ–protective layer materials such as SrO[4–6], SrCaO[4,5,7], and CaO[8] are used next to reduce the firing voltage. An important problem is that these materials are highly reactive to H_2O and CO_2. In a conventional manufacturing process, the protective layer deposited in a vacuum chamber is exposed once to ambient air. Long-term panel aging must stabilize firing voltage[4]. Several reports have described that panel annealing at lower pressures is effective for decreasing the firing voltage[9–13]. In the case of MgO, vacuum annealing increased the γ value because of the surface cleaning effect[14].

In this study, we examined the panel processing in high vacuum (pressure range 10^{-6} Pa) after deposition of the protective layer. This is applicable to high γ material as well as MgO. In the case of MgO, we demonstrate that the aging time is significantly shortened and that the discharge time lag is greatly improved compared with that of a conventional manufacturing method. The evacuation pressure effect on the sealing process is discussed quantitatively.

2. Experimental

Our new equipment is depicted schematically in **Fig. 1**. Front and rear panels were transferred automatically to each vacuum chamber, such as the evaporation chamber and sealing chamber, by a robot hand set in the transportation chamber. Front and rear panels were sealed in a sealing chamber after protective layer deposition. The rear pane l was degassed sufficiently in loading and unloading (L/UL) chamber 2 before sealing (prebaking process of real panels). Discharge gas was filled in the panel through a hole in the rear panel. Then the hole was closed with an indium cap in the gas filling–sealing chamber. It is noteworthy that all panel transfer and sealing was done in high vacuum.

Figure 2 shows a flow chart of processing conditions of panels of three kinds. Panel 1 (conventional panel) was sealed in ambient air and evacuated to eliminate

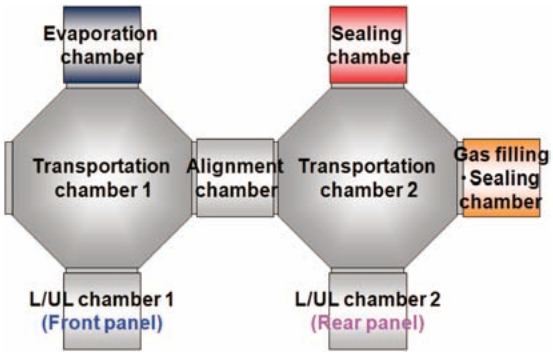

Fig. 1 Our new equipment for AC–PDP manufacturing.

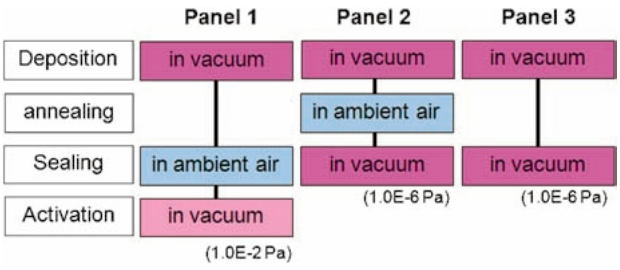

Fig. 2 Panel processing conditions.

†1 Present Address: Department of Electronics, Kyushu University, 744 Motooka, Nishi-ku, Fukuoka, 819–0395, Japan

Table 1 Specifications of the test panel and driving waveform.

■Specifications of the test panel

Vertical pitch	440 μm
Horizontal pitch	230 μm
Gap between electrodes	80 μm
Thickness of dielectric layer	30 μm
Height of rib	130 μm
Thickness of protective layer	500 nm
Discharge gas	Ne–Xe 20%, 67 kPa

■Driving waveform (continuous)

Period of pulse	15 kHz
Width of pulse	32 μs (50% duty ratio)

H_2O and CO_2 from the MgO surface. To stabilize the panel performance (activation process), the vacuum evacuation is absolutely necessary in a conventional process. Even after vacuum evacuation for 5 hr, the pressure in the Panel 1 before gas filling cannot be lower than 10^{-2} Pa at the sealing hole because of the low conductance of the evacuation glass tube. To clarify the effect of the high vacuum activation on the discharge characteristics, the panel annealed at the same condition as Panel 1 was sealed at 10^{-6} Pa (Panel 2). Panel 3 was processed in high vacuum to keep the MgO surface as clean as possible (''all-in-vacuum'' panel).

Specifications of the test panel and driving waveform are presented in **Table 1**. The X and Y electrodes of the PDP front panel are strips of 180 μm width. The inter-electrode distance between the X and Y electrodes is 80 μm. The display area is 50×50 mm^2. The MgO thin films are deposited up to 500 nm using an electron beam evaporation method on the dielectric layer (30 μm) covering the X and Y electrodes. The following deposition conditions were used: substrate temperature of 523 K, deposition rate of 0.5 nm/s, and a certain amount of oxygen gas in the evaporation chamber. The X-ray diffraction (XRD) pattern of the deposited MgO–thin film shows a (111) preferred orientation. The rear panel of PDP has stripe ribs of 130 μm height. Three colors of phosphors are deposited: red ((Y, Gd, Eu)BO_3), green (Zn_2SiO_4:Mn), and blue ((Ba, Eu)$MgAl_{10}O_{17}$). The PDP are filled with Ne–Xe (20%) gas of 67 kPa for vacuum ultraviolet (VUV) radiation from the dielectric barrier discharge.

Panel characteristics such as discharge voltage (V_{f1}, V_{fn}, $V_{s\,max}$, and $V_{s\,min}$), luminance, and discharge time lag were measured at room temperature. The maximum firing voltage (V_{fn}) and minimum firing voltage (V_{f1}) are defined respectively as the voltages applied between X and Y electrodes when the last and first cell turns on. The maximum sustain voltage ($V_{s\,max}$) and minimum sustain voltage ($V_{s\,min}$) are defined respectively as the voltages applied between X and Y electrodes when the first and last cell turns off. PDP is usually operated between V_{f1} and $V_{s\,max}$. The luminance, luminous efficacy and discharge time lag were measured in the static margin (between V_{f1} and $V_{s\,max}$). The discharge voltage and current were measured using a current probe (PC5000a; Sanwa Electric Instrument). The luminance was measured using a luminance meter (LS–100; Konica Minolta Holdings Inc.). The luminous efficacy (η) was calculated from the equation $\eta = \pi LS/P$, where π, L, S, and P respectively represent the ratio of circumference of a circle to its diameter, the luminance, the luminous area, and the power of discharge.

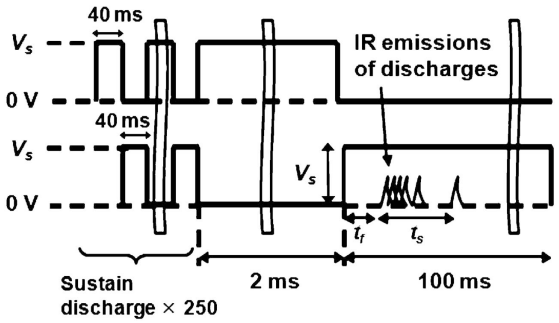

Fig. 3 Applied waveform cycle for t_f and t_s measurements.

Figure 3 shows the applied waveform cycle for the discharge time lag measurement, where the discharge time lag consists of the formative time lag (t_f) and statistical time lag (t_s). The upper and lower waveforms were applied respectively to the X and Y electrodes of the front panel. First, 250 pulses were applied to a pair of surface discharge electrodes. After 2 ms as a period of nondischarge time, a sustained pulse was applied to electrodes again for measuring the discharge time lag. The discharge time lag between the applied measurement pulse and the discharge emission was measured 1000 times. The discharge emission was measured using an avalanche photodiode (C5460; Hamamatsu Photonics KK).

3. Results and Discussion

Figure 4 portrays the maximum firing voltage (V_{fn}) shown as a function of aging time for Panels 1, 2, and 3. The V_{fn} of Panels 2 and 3 were stabilized in only 15 min, whereas that of Panel 1 was stabilized in 120 min. The result underscores that the high vacuum activation is effective for decreasing the aging time. **Figure 5** shows the discharge voltage data of Panels 1, 2, and 3. The V_{f1} of Panel 2 was 15 V lower than that of Panel 1. The result indicates that high vacuum activation is effective for decreasing not only the aging time but also the firing voltage. Results also revealed that the discharge voltage of Panel 3 was slightly lower than that of Panel 2. The result proves that the firing voltage of the panel sealed in ambient air do not return to the same as that of the ''all-in-vacuum'' panel by the high vacuum activation.

Figure 6(a) and **6(b)**, respectively show the luminance and luminous efficacy as a function of the sustaining voltage for Panels 1, 2, and 3. No significant difference was found among them. The luminance and luminous efficacy depend only on the sustaining voltage. Based on this result, we can understand that the VUV radiation in-

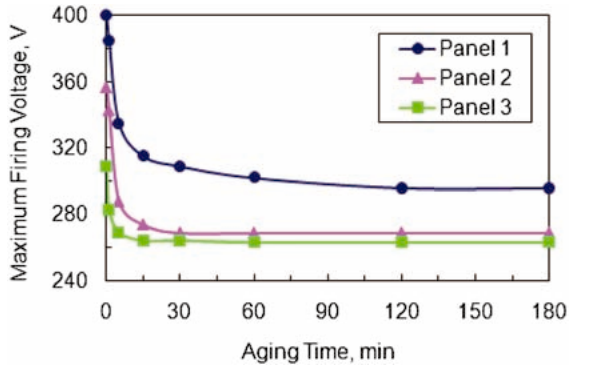

Fig. 4 Aging time dependence of the maximum firing voltage (V_{fn}).

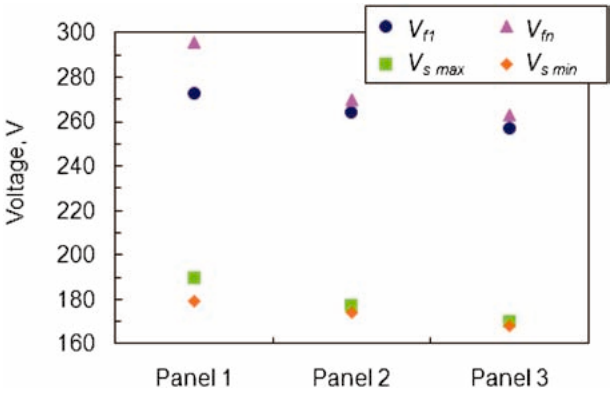

Fig. 5 Discharge voltage of Panels 1, 2, and 3.

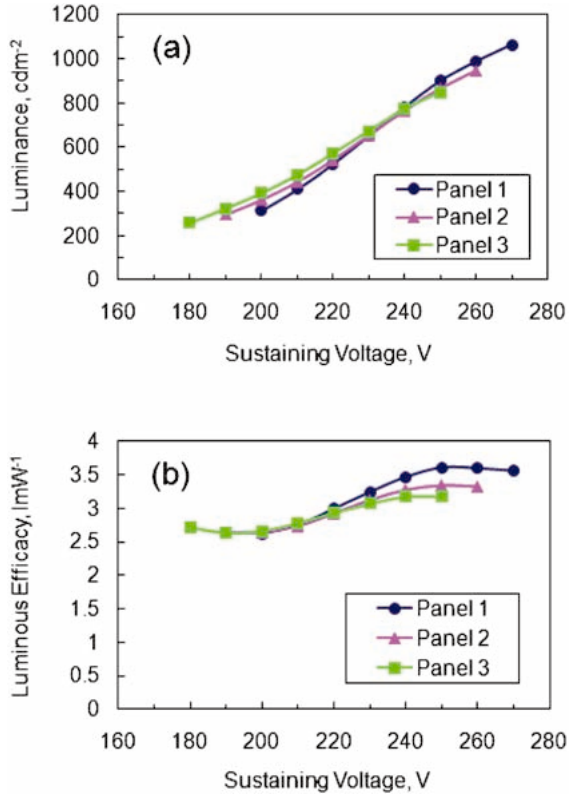

Fig. 6 (a) Luminance and (b) luminous efficacy of Panels 1, 2, and 3.

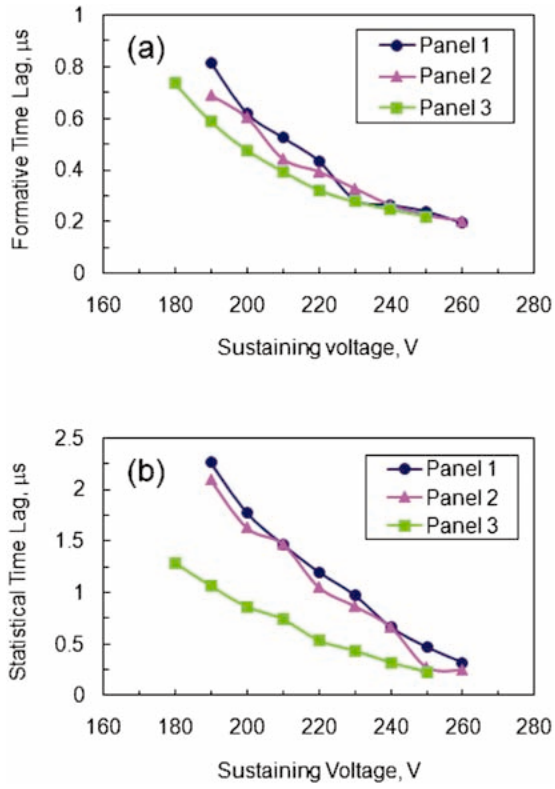

Fig. 7 (a) Formative time lag and (b) statistical time lag of Panels 1, 2, and 3.

tensity from discharge has no influence on the manufacturing process.

Figure 7(a) and **7(b)** respectively present the formative and statistical time lag as a function of the sustaining voltage for Panels 1, 2, and 3. The statistical time lag of Panel 3 decreased drastically to half that of Panel 1. The result of the ''all-in-vacuum'' panel agrees with that of the vacuum sealing method[15]. In the vacuum sealing method, although the MgO layer was once exposed to ambient air, the panel was sealed in a vacuum chamber at 10^{-3} Pa. However, the statistical time lag of Panel 2 was the same as that of Panel 1. The result proves that the statistical time lag is increased by annealing in ambient air. It must be emphasized that the high vacuum activation does not decrease the statistical time lag.

Finally, we investigated the effect of rear panel pre-baking temperature on a discharge time lag in the ''all-in-vacuum'' method. The pre-baking process is important because the rear panel emits many impurities in the high-vacuum sealing process. **Figure 8(a)** and **8(b)** respectively depict formative and statistical time lags as a function of the sustaining voltage for the ''all-in-vacuum'' panels manufactured with three pre-baking temperatures. The pre-baking temperature of Panel 3 was 773 K. A close relation is apparent between the pre-baking temperature and the statistical time lag: a shorter discharge time lag is achieved at higher pre-baking temperatures. The result indicates that the statistical time lag is extremely sensitive to contamination.

Our experiment underscores that sealing in high vacuum (Panels 2 and 3) is effective for decreasing aging time

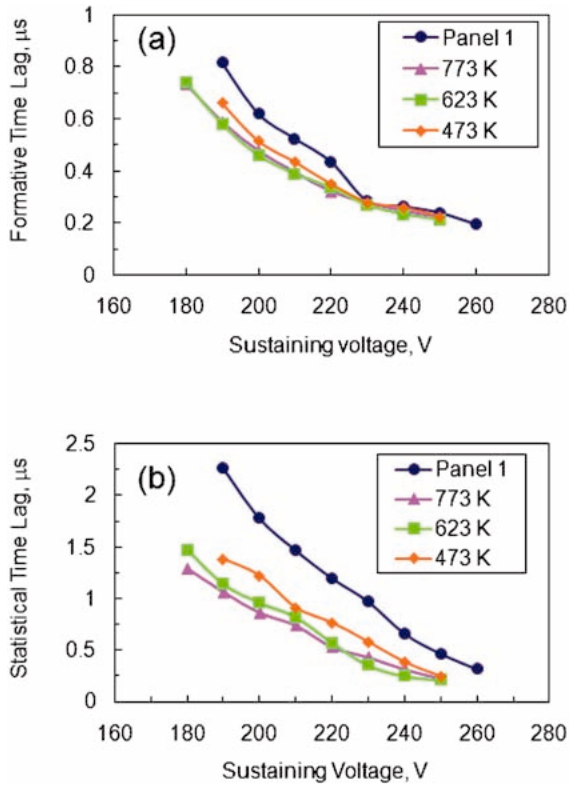

Fig. 8 (a) Formative time lag and (b) statistical time lag of the ''all-in-vacuum'' panels manufactured with different pre-baking temperatures.

and firing voltage. However, the statistical time lag is not decreased merely by sealing in high vacuum. A statistical delay time lag is widely known to follow the distribution reported by Laue in 1925[16]. Actually, $N_t/N_0 = \exp(-iPt)$, where N_t/N_0 is the fraction of delay times greater than t, i is the rate of appearance of free electrons, and P is the breakdown probability that an electron initiates breakdown. The average statistical delay time t_s equals $1/(iP)$. It has been demonstrated that the major free electrons in ac-PDP are exoelectrons[17]. In our experiment, Panel 2 and Panel 3 have almost identical P values because there are few discharge gas impurities and little MgO surface contamination. Therefore, we can discuss t_s from the perspective of i related to the characteristics of exoelectron emission from MgO surface. Our experiment clearly illustrates that Panel 2 has longer t_s, which corresponds to a small i value: a lower rate of appearance of exoelectrons. The MgO surface of Panel 2 reacted on chemically H_2O and CO_2 by annealing in ambient air, which influenced exoelectron emission characteristics. Furthermore, we must emphasize that the exoelectron emission characteristics of the MgO annealed in ambient air never return after high vacuum activation (pressure range 10^{-6} Pa).

4. Summary and Conclusions

We produced panels of three kinds and evaluated the effect on panel characteristics of keeping the MgO surface clean and eliminating adsorbed materials. Results show that the aging time depends on the activation pressure. It is possible to shorten the statistical time lag by processing a panel in high vacuum. The statistical time lag is increased by annealing in ambient air. It is not decreased by high vacuum activation. Results show that our ''all-in-vacuum'' process is effective for PDP manufacturing, even when using a MgO protective layer.

References

1) H. Uchiike, K. Miura, N. Nakayama, T. Shinoda and Y. Fukushima: IEEE Trans. Electron Devices, **11** (1976) 1211.
2) T. J. Vink, A. R. Balkenende, R. G. F. A. Verbeek, H. A. M. van Hal and S. T. de Zwart: Appl. Phys. Lett., **80** (2002) 2216.
3) M. F. Gillies and G. Oversluizen: J. Appl. Phys., **91** (2002) 6316.
4) T. Shinoda, H. Uchiike and S. Andoh: IEEE Trans. Electron Devices, **26** (1979) 1163.
5) G. Uchida, S. Uchida, H. Kajiyama and T. Shinoda: J. Appl. Phys., **106** (2009) 09331.
6) Ki-Woong Whang, Tae-Ho Lee and Hee-Woon Cheong: *Proceedings of Society for Information Display 2010 International Symposium* (Seattle, 2010) p. 732.
7) Y. Motoyama, Y. Murakami, M. Seki, T. Kurauchi and N. Kikuchi: IEEE Trans. Electron Devices, **54** (2007) 1308.
8) M. Sakai, S. Hatta, Y. Fukui, Y. Honda, M. Okafuji, Y. Yamauchi, M. Nishitani and Y. Takata: *Proceedings of the 15th International Display Workshops* (Niigata, Japan, 2008) p. 1881.
9) M. Lenzen, G. M. Turner and R. E. Collins: J. Vac. Sci. Technol. A, **17** (1999) 1002.
10) K. Akaishi, K. Ezaki, T. Kubota and O. Motojima: Vacuum, **53** (1999) 285.
11) S. Uchida, H. Sugawara, Y. Sakai, T. Watanabe and B. H. Hong: J. Phys. D, **33** (2000) 62.
12) H. R. Han, Y. J. Lee and G. Y. Yeom: J. Vac. Sci. Technol. A, **19** (2001) 1099.
13) S. J. Kwon and C. K. Jang: J. J. Appl. Phys., **45** (2006) 804.
14) J. K. Kim, K. S. Moon, K. W. Whang and J. H. Lee: J. Vac. Sci. Technol. B, **19** (2001) 687.
15) C. S. Park, H. S. Tae, Y. K. Kwon and E. G. Heo: IEEE Trans. Electron Devices, **54** (2007) 1315.
16) M. v. Laue: Ann. Phys., **381** (1925) 261.
17) S.-H. Yoon, H.-W. Ryu, C.-R. Hong, D.-H. Kim, J.-J . Ko and Y.-S. Kim: *Proceedings of Society for Information Display 2008 International Symposium* (Los Angeles, CA, 2010) p. 287.